3.6

COMPRESSED AIR TUNNEL FLOW VISUALISATION OVER TORPEDO SHAPED BODIES FOR SELF NOISE EVALUATION

G J Burrows

Admiralty Underwater Weapons Establishment
Portland Dorset

Introduction

1. Torpedo self noise is the acoustic noise that is generated by the torpedo in passing through the water and received by the torpedoes own homing sensor mounted in the nose of the torpedo. Self noise represents a background interference which limits the homing performance of the torpedo.

2. A primary source of self noise is flow noise which emanates from a transition point at which water flow over the torpedo nose changes abruptly from laminar to turbulent flow. The position at which this flow transition occurs directly influences the self noise level received by the torpedoes homing sensor and thus the overall performance of the torpedo. A knowledge of the parameters influencing the position at which flow transition occurs is, therefore, important in optimising torpedo performance.

3. Numerous theoretical methods have been developed to predict the location of flow transition (reference 1-4). Figure 1 shows a typical plot of Pressure Coefficient (Cp) against nondimensional torpedo length on which has been superimposed locations of flow transition for a particular torpedo speed that have been derived from several established theoretical prediction methods. Unfortunately, as can be seen, when the methods are applied to the bluff shape of a torpedo body, widely differing locations for transition are obtained.

4. A flow visualisation technique has been developed to determine experimentally the location of flow transition for different torpedo body shapes over a range of typical Reynolds numbers and to provide data to establish a reliable theoretical flow transition prediction method.

5. Compressed Air Tunnel

The flow visualisation technique described uses the unique facilities of the compressed Air Tunnel (CAT) at the National Physical Laboratory, Teddington. The CAT facility allows a full scale torpedo body to be mounted inside the tunnel and to be run at an equivalent in-water torpedo speed (on a Reynolds number basis) up to 126 knots. Normal operating flow characteristics of torpedoes may thus be obtained without the problem of having to scale or extrapolate results.

6. Figure 2 shows a cross sectional plan view of the CAT. The tunnel consists of a 1.83 m (6.0 ft) diameter open jet working section and an annular return circuit, the whole being enclosed in a pressure shell. The maximum working pressure is 25 atmospheres absolute and has a maximum air speed (of 27.4 m/s (90 ft/s). A two-bladed fan is driven by a 298kw, 800 rpm electric motor.The rms pressure fluctuation levels in the CAT have been measured to be 0.3% rising to 0.6% at maximum speed and pressure. The torpedo body was rigidly fixed in the centre of the CAT working section by two streamline struts. Preset adjustments of the aft strut enabled various angles of attack to be obtained. A Television camera was mounted inside the CAT (in the stagnant flow region), with a television monitor and video recorder located outside the CAT for observation/recording during tunnel operation.

7. Flow Visualisation Technique

A paint suspension, consisting of Paraffin, Diesel Oil, Oleic Acid and fine (less than 0.1μm, 4μ inches) Titanium Dioxide "day-glow" particles, was carefully applied to the torpedo body in the CAT.

8. The tunnel was then pressurised and run for several minutes. Air flow over the body produced surface flow patterns corresponding to flow regimes present in the boundary layer.

9. The formation of these flow patterns was primarily governed by two effects:

a. A migration and deposition of the very fine Titanium Dioxide particles

b. A drying action in the paraffin base which was directly related to the energy present in the boundary layer.

10. Immediately following a run, the CAT was returned to atmospheric pressure and the torpedo body was irradiated with strong ultra-violet light. The resulting striae and wet and dry contrast areas fluoresced enabling high contrast photographic records of the flow patterns to be obtained.

11. The interpretation of the flow patterns was based upon the migratory streaks and deposition of the titanium dioxide particles, their direction convergence, divergence or disappearance and of the relative contrast of the wet and dry areas over the body. The convergence of the lines in the direction of flow implied flow separation, the divergence of lines in the direction of flow implied flow attachment. The disappearance of lines was associated with either extensive flow separation or turbulence. High contrast areas (where the paraffin oil base had dried) was associated with turbulent flow and low contrast areas (paraffin oil base still wet) was associated with laminar flow.

12. A mathematical analysis by Squires (Reference 5) indicates that the effect of the oil based paint on the boundary layer is very small, and in the worst case would result in the position of separation/transition changing by less than 2%.

13. Reynolds Number Scaling

The torpedo body was run in compressed air at the same free stream Reynolds number as the actual torpedo would experience in sea water.

$$\text{Reynolds number, } Re = \frac{\rho V d}{\mu}$$

$$\text{Thus } \frac{V_f \cdot d_f}{(\mu/\rho)_{water}} = \frac{V_m \cdot d_m}{(\mu/\rho)_{\text{air at n atmospheres}}}$$

where; V = Velocity
d = Characteristic dimension
μ = Absolute Viscosity
ρ = Density
f = Full Scale
m = Model Scale

Hence, since model and full scale torpedo bodies are identical:

$$V_f = V_m \left(\frac{\mu \text{ water}}{\mu' \text{ air}}\right) \cdot \left(\frac{\rho' \text{ air}}{\rho \text{ water}}\right)$$

where now prime indicates values at an absolute pressure of n atmospheres.

Ths viscosity changes by a negligible amount over the range of pressures involved, hence;

$$V_f = V_m \cdot n \left(\frac{\mu \text{ water}}{\mu \text{ air}}\right) \left(\frac{\rho' \text{air}}{\rho \text{ water}}\right)$$

The following are typical values for Viscosity and Density:

Viscosity:

Air (Atmospheric pressure and 20°C)	18.20×10^{-6} Pa.s
Sea Water (35‰ Salinity, 10°C)	1.480×10^{-3} Pa.s

Density:

Air (Atmospheric pressure and 20°C)	1.197 $kg.m^{-3}$
Sea Water (35‰ Salinity, 10°C)	1027 $kg.m^{-3}$

Thus: $V_f = 0.0948\ V_m \cdot n$

By varying Vm or n (maximum values of 27.4 m/s and 25 atmospheres respectively) values of V_f could be obtained up to 64.9 m/s (126 knots).

14. Results

Figures 3-5 show side views of the flow patterns on the torpedo body for three different torpedo speeds. When the torpedo body was run at a low equivalent torpedo speed, laminar flow separation occurred, as shown in Fig 3. A large separation bubble, about 30mm in extent, developed and the reverse flow could be observed from the television monitor. The flow re-attached itself to the body further aft and developed into fully turbulent flow.

15. Figure 4 shows the same torpedo body run at a higher equivalent torpedo speed. The dark band indicates the transition from Laminar to turbulent flow. This figure also shows a number of wedges of premature turbulent flow. The wedges have been caused by surface discontinuities and roughnesses that are comparable to the boundary layer thickness over the body. The wedges of turbulent flow are detrimental in prematurely raising the torpedo self noise level.

16. Raising the equivalent torpedo speed even higher for the same torpedo body results in the flow pattern of Figure 5. A large number of premature turbulent flow wedges developed to such an extent that the natural flow transition location was not discernable. Transverse, circumferential, dark bands can also be seen on this figure. These dark bands are surface "high spots" and are machining errors in the torpedo body profile. These surface "high spots" are contributory in the promotion of premature wedges of turbulent flow.

17. Figure 6 shows the magnified error of the accurately measured torpedo body profile superimposed on the theoretical torpedo profile. The transverse "hatched" bands represent the dark bands observed from the flow visulisation patterns, and one can see the high correlation between high spots and transverse body bands.

18. Subsequent analysis of the flow visualisation results has revealed that the Michel theoretical flow transition prediction method produces good agreement with the flow visualisation results.

19. Stratford's method (Reference 6) of predicting the location of flow separation gives good agreement with the observed flow visualisation separation results.

REFERENCES

1. Van Driest, E R and Blumer C B Boundary Layer Transition, AIAA Journal, Vol 1, No 6, 1963

2. Granville P S. The calculation of Viscous Drag on Bodies of Revolution, David Taylor Model Basin Report, 849, 1953.

3. Michel R, Etede de la Transition sur les Profiles d'aile; Establishment d'un critere de Determination de Point de Transition et Calcul de la Trainee de Profile. Incompressible, ONERA Report 1/1578A, 1951

4. Smith, AMO and Gamberoni N., Transition, Pressure Gradient, and Stability Theory, Douglas Aircraft Company, Report ES 26388, 1956.

5. Squire, LC., The Motion of a thin oil sheet under the Boundary Layer of a Body, AGARDOGRAPH No 70, 1962.

6. Stratford B S Aeronaut, Res. Council, London RM-3002, 1954

DH

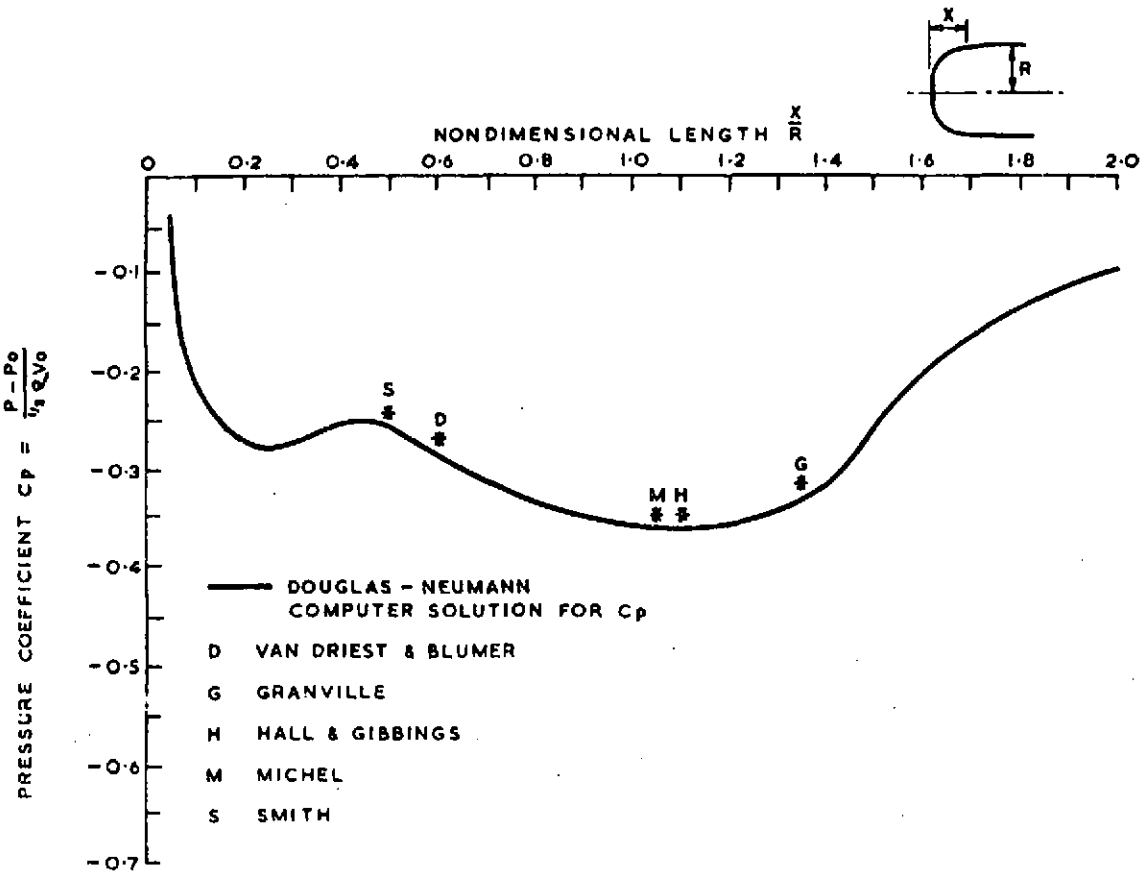

FIG. 1. PREDICTED TRANSITION FOR TORPEDO NOSE

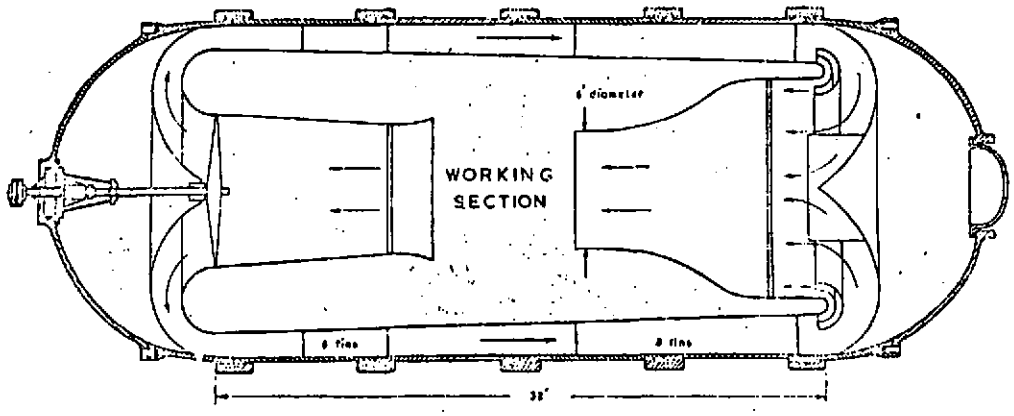

FIG. 2. Plan view of Compressed Air Tunnel.

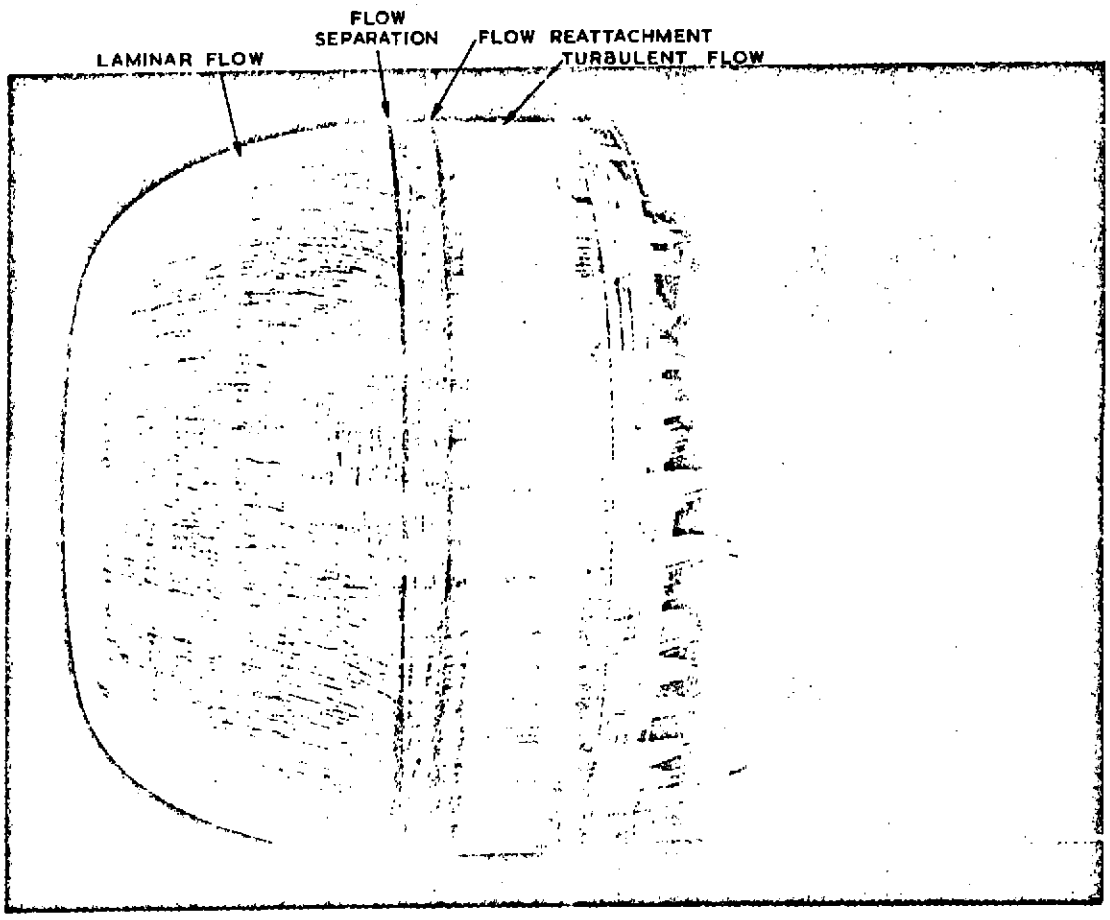

FIG.3 TORPEDO BODY FLOW VISUALISATION PATTERN - LOW SPEED

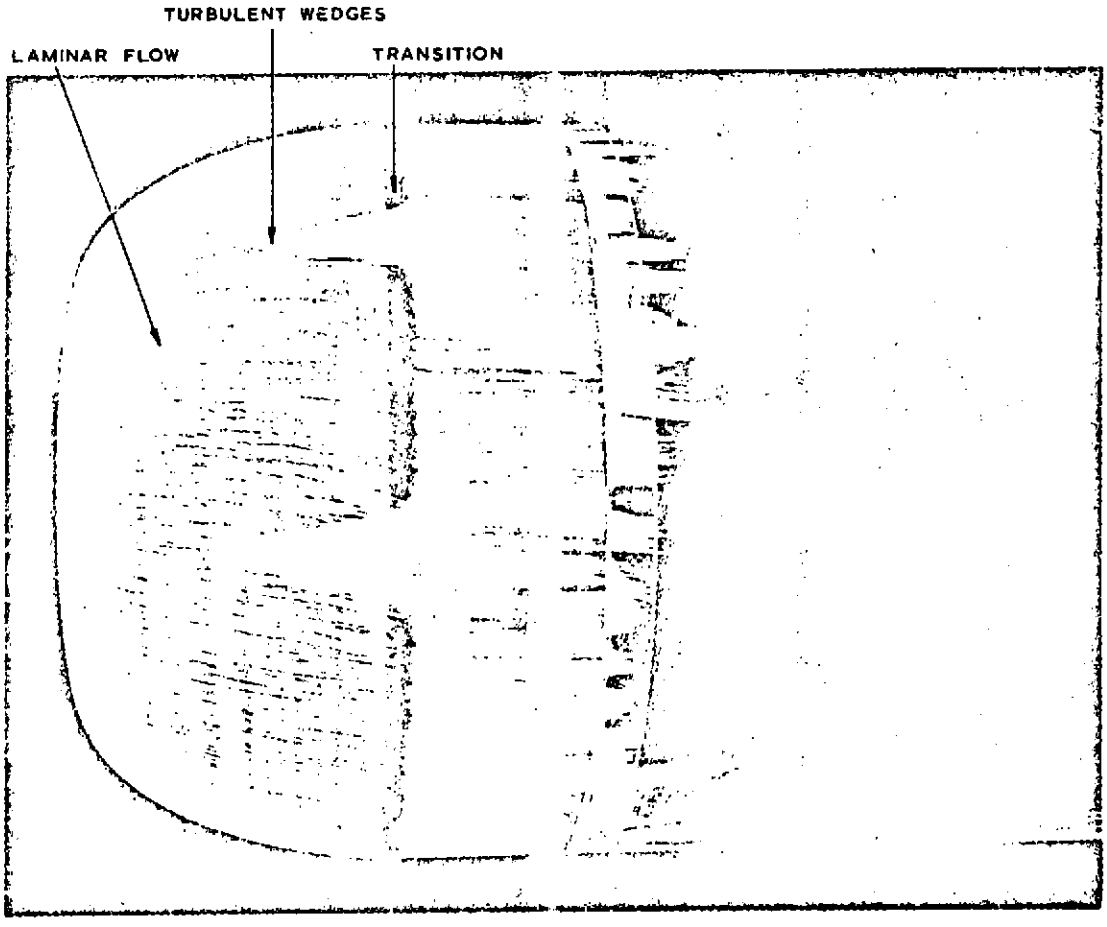

FIG.4 TORPEDO BODY FLOW VISUALISATION - MEDIUM SPEED

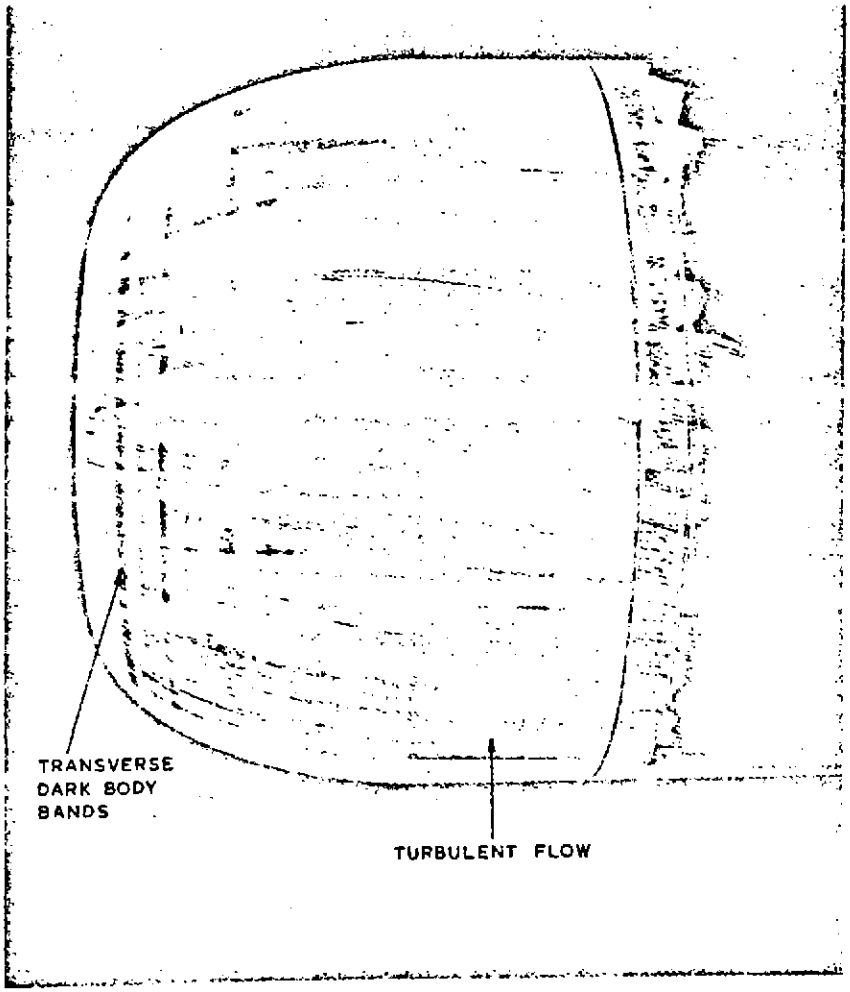

FIG.5 TORPEDO BODY FLOW VISUALISATION - HIGH SPEED

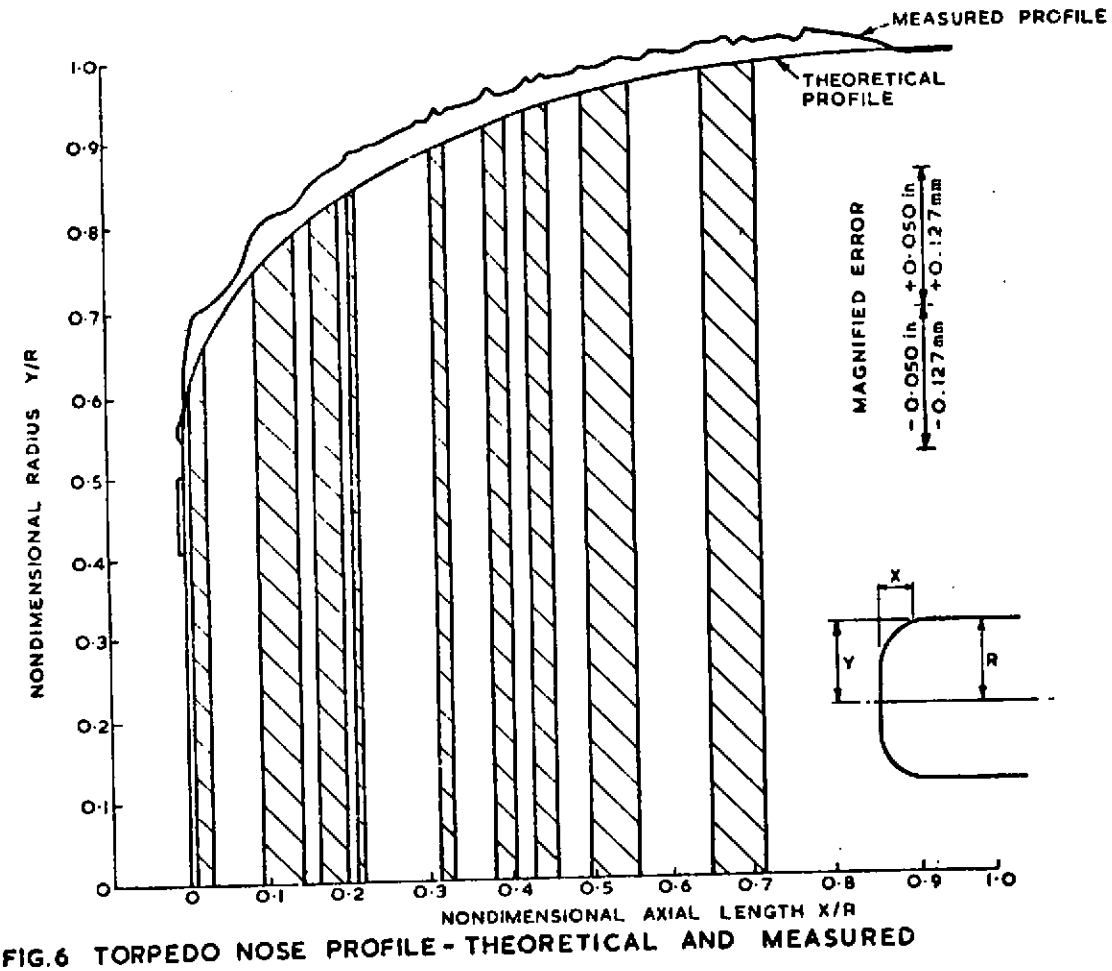

FIG.6 TORPEDO NOSE PROFILE - THEORETICAL AND MEASURED